Metallizing the Mott insulator TiOCl by electron doping

2006 J. Phys.: Condens. Matter 18 10943

(http://iopscience.iop.org/0953-8984/18/48/021)

INSTITUTE OF PHYSICS PUBLISHING JOURNAL OF PHYSICS: CONDENSED MATTER

J. Phys.: Condens. Matter **18** (2006) 10943–10953 doi:10.1088/0953-8984/18/48/021

Metallizing the Mott insulator TiOCl by electron doping

L Craco[1], **M S Laad**[2] **and E Müller-Hartmann**[1]

[1] Institut für Theoretische Physik, Universität zu Köln, 77 Zülpicher Straße, 50937 Köln, Germany
[2] Department of Physics, Loughborough University, LE11 3TU, UK

Received 26 January 2006, in final form 4 October 2006
Published 17 November 2006
Online at stacks.iop.org/JPhysCM/18/10943

Abstract

Based on recent experiments, we describe the Mott insulating, but undimerized, state of TiOCl using the local-density approximation combined with multi-orbital dynamical mean field theory (LDA + DMFT) for this $3d^1$ system. Good agreement with the high estimated value of the superexchange is obtained. The possibility of an electron-doped insulator–metal transition in TiOCl is investigated in this scheme and a Mott–Hubbard transition with a jump in carrier density *inside* the metallic state is found. Clear, coincident, discontinuous changes in orbital occupations are observed, showing that such a transition would involve strong, multi-orbital correlations. These results call for studies on suitably intercalated TiOCl that may induce metallization and, possibly, unconventional superconductivity.

(Some figures in this article are in colour only in the electronic version)

1. Introduction

Titanium-based oxide systems have recently been found to exhibit varied physical properties. Being electron-doped analogues ($3d^1$) of the well-known high-T_c superconductors, they have been studied with a view to search for superconductivity. Titanium oxychloride (TiOCl) is of special interest in this context [1]: it is a layered material undergoing spin–Peierls dimerization at low T. Unlike other candidate spin–Peierls systems like $CuGeO_3$, the superexchange scale $J \simeq 660$ K in TiOCl is almost an order of magnitude larger. Additionally, the fact that the single d electron resides in the t_{2g} orbitals might suggest the absence of Jahn–Teller effects, implying weakened tendency for doped carriers to localize. It has nevertheless proved to be difficult to dope TiOCl using traditional techniques. However, structurally similar materials such as Li-intercalated ZrNCl are known to undergo an insulator–metal transition and exhibit superconductivity [2], leaving the issue open for TiOCl.

Early observation of spin-gap generation in spin susceptibility showing a kink at 94 K and an exponential drop below $T_d = 66$ K, accompanied by a doubling in the unit cell along b, suggested a spin–Peierls dimerized state in TiOCl [3]. These effects were recently confirmed

by temperature-dependent x-ray diffraction. This experiment shows the existence of a phase transition at $T_{c2} = 90$ K, corresponding to a lowering of the lattice symmetry [4]. Furthermore, below $T_{c1} = 66$ K a two-fold superstructure develops, indicating the formation of spin-singlet pairs via direct exchange between neighbouring Ti atoms. That this may in fact involve coupled spin, orbital and lattice degrees of freedom is suggested by large phonon anomalies [5] and by T-dependent g-factors and ESR linewidths [6]. This should not be too surprising: in fact, the magnetism of early transition metal oxides (TMOs) is known to be sensitively determined by the above factors [7]. Indeed, various groups have recently studied the electronic structure of TiOCl [8–11]: in contrast to what is expected from a cubic crystal field, the low-symmetry crystal field in TiOCl splits the t_{2g} orbitals into a lower-lying d_{xy} orbital and higher-lying $d_{yz,zx}$ orbitals. The lone electron in TiOCl would then occupy the lowest d_{xy} orbital at low T. However, the higher-lying $d_{yz,zx}$ orbitals are only about 0.2 eV above the lowest one, and, in a situation where the LDA bandwidth is about 2.5 eV, strong inter-orbital mixing can be expected. How the system manages to achieve a spin–Peierls insulating state when moderately strong, multi-orbital Coulomb interactions in the d shell are switched on is a major question for *ab initio* theoretical approaches.

In this work, we aim to address precisely this issue in part. Starting with the LDA calculation for the actual structure of TiOCl, we explicitly treat the dynamical effects of strong, multi-orbital electronic correlations in the $3d^1$ case using multi-orbital dynamical mean field theory (DMFT). To solve the DMFT equations, we employ the multi-orbital iterated perturbation theory (IPT) used successfully earlier [12]. This is in fact necessary: the LDA generically gives metallic states owing to neglect of strong electron correlations, while LDA + U, which does give the correct *ground* state(s) for insulating systems, generically overestimates localization, leading to charge gap(s) too large compared to experiment. Moreover, being ground state theories, both are incapable of accessing the ubiquitous dynamical spectral weight transfers in response to various small perturbations; the importance of such aspects is known to be crucial, e.g., in insulator–metal transitions. This characteristic underlying the ill-understood response of correlated systems can however be understood within DMFT and its extensions.

2. Methodology

TiOCl crystallizes in the $Pmmn$ space group at high T, and consists of bilayers of Ti^{3+} and O^{2-} parallel to the ab plane separated by Cl^- layers. In a perfect octahedral environment the crystal field would split the atomic d levels into three-fold degenerate (t_{2g}) and doubly degenerate e_g levels. However, the basic $TiCl_2O_4$ unit in TiOCl is distorted, and the low-symmetry crystal field in the real structure splits the t_{2g} degeneracy, with the lowest d_{xy} orbital separated from slightly higher-lying $d_{yz,zx}$ orbitals. In this work we employ the LDA density of states (DOS) obtained by Saha-Dasgupta *et al* [11] using the full potential minimum bases local orbital code (FPLO) [13] to perform our LDA + DMFT calculations. Following previous calculations by Seidel *et al* [8] on the same compound, the coordinate system has been chosen as $\hat{z} = a$ and the $\hat{x}$ and $\hat{y}$ axes rotated 45° relative to b and c axes. The inset of figure 1 shows the one-electron DOS obtained using density-functional calculations in the LDA. As expected, the LDA does not give an insulating solution. The LDA occupations of each of the t_{2g} orbitals are $(n_{xy}, n_{yz}, n_{zx} = 0.54, 0.23, 0.23)$. Clearly, the occupation of each orbital is far from integral, and only the *total* t_{2g} occupation per Ti site is constrained to be $(1 + x)$ with $x = 0$ for pure TiOCl. This discussion clearly shows that strong multi-orbital correlations are *necessary* to drive a Mott insulator in this $3d^1$ system.

We now show how LDA + DMFT reconciles this problem, yielding not only the correct ground state, but also a quantitative picture for the one-electron (hole) excitation spectrum. The

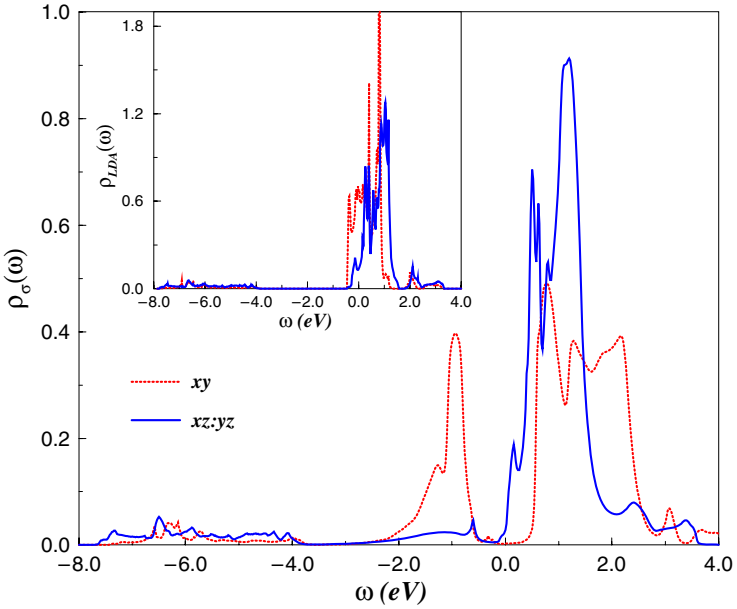

Figure 1. LDA + DMFT and LDA (inset) partial densities of states (DOSs) for TiOCl. The dotted (red) line denotes the DOS for the non-degenerate ground-state (xy) orbital, the full (blue) line denotes the DOS for the higher-lying (two-fold degenerate) t_{2g} orbitals. Higher-lying e_g and O 2p bands are not shown.

LDA Hamiltonian is

$$H_0 = \sum_{k,\alpha\beta} \epsilon_k^{\alpha\beta} c_{k\alpha\sigma}^{\dagger} c_{k\beta\sigma} + \sum_{i,\alpha\sigma} \epsilon_{i\alpha\sigma}^{0} n_{i\alpha\sigma}, \tag{1}$$

where $\epsilon_{i\alpha\sigma}^{0} = \epsilon_{i\alpha\sigma} - U(n_{\alpha\bar{\sigma}} - \frac{1}{2}) + \frac{J_H}{2}\sigma(n_{\alpha\sigma} - 1)$ with U and J_H as defined below. The second term above takes care of avoiding the double-counting of interactions already treated on the average by the LDA.

We account for strong multi-orbital correlations in TiOCl by choosing the intra-orbital U, the local Hund coupling J_H and the inter-orbital $U_{\alpha\beta} \equiv U' \simeq U - 2J_H$. We stress the importance of including U': indeed, neglecting U' would imply that an electron hopping from site i to its neighbour (avoiding the same lowest orbital to escape the penalty of U) would occupy the slightly higher-lying $d_{yz,zx}$ orbitals. With $U' = 0$, and a one-electron band-width of 2.0 eV, this electron (and the hole it leaves behind on the site i) would hop freely, always giving a *metallic* state. The full many-body Hamiltonian is

$$H = H_0 + U \sum_{i\alpha} n_{i\alpha\uparrow} n_{i\alpha\downarrow} + U' \sum_{i\alpha\beta\sigma\sigma'} n_{i\alpha\sigma} n_{i\beta\sigma'}. \tag{2}$$

For early TMOs, it is sufficient to consider only the t_{2g} bands in the LDA + DMFT scheme[3]. Due to t_{2g}–e_g and t_{2g}–2p hybridization in the real crystal structure of TiOCl, we include the TM e_g and O 2p parts (of the DOS) with 't_{2g}' symmetry in the unperturbed band DOS. Further, in the paramagnetic/ferro-orbital situation (see below) applicable to TiOCl in the undimerized state, we have $G_{\alpha\beta\sigma\sigma'} = \delta_{\alpha\beta}\delta_{\sigma\sigma'}G_{\alpha\sigma}(\omega)$ and $\Sigma_{\alpha\beta\sigma\sigma'}(\omega) = \delta_{\alpha\beta}\delta_{\sigma\sigma'}\Sigma_{\alpha\sigma}(\omega)$. The DMFT solution in the t_{2g} sector involves (i) replacing the lattice model by a multi-orbital,

[3] The O 2p bands and the TM e_g bands are well separated from the TM e_g bands in early TMOs.

asymmetric Anderson impurity model, along with (ii) a self-consistency condition which requires the impurity propagator to coincide with the local Green's function of the lattice, given by

$$G_\alpha(\omega) = \frac{1}{V_B}\int \mathrm{d}^3k\left[\frac{1}{(\omega+\mu)1 - H^0_{\mathrm{LDA}} - \Sigma_\alpha(\omega)}\right]_\alpha. \tag{3}$$

Further, U', J_{H} scatter electrons between the d_{xy} and $\mathrm{d}_{yz,zx}$ bands, so only the total number, $\sum_\alpha n_{\mathrm{t}^\alpha_{2g}}$, is conserved in accord with Luttinger's theorem.

To solve the multi-orbital single-impurity problem, we use the multi-orbital (MO) IPT, suitably generalized for arbitrary band-filling and temperatures. Explicitly, we have

$$\Sigma_\alpha(\omega) = \frac{\sum_\gamma A_{\alpha\gamma}\Sigma^{(2)}_{\alpha\gamma}(\omega)}{1 - \sum_\gamma B_{\alpha\gamma}\Sigma^{(2)}_{\alpha\gamma}(\omega)} \tag{4}$$

where, $\Sigma^{(2)}_{\alpha\gamma}(\mathrm{i}\omega) \equiv \frac{U^2_{\alpha\gamma}}{\beta^2}\sum_{n,m} G^0_\alpha(\mathrm{i}\omega_n)G^0_\gamma(\mathrm{i}\omega_m)G^0_\gamma(\mathrm{i}\omega_n + \mathrm{i}\omega_m - \mathrm{i}\omega)$ and $G^0_\alpha(\omega) = [\omega + \mu_\alpha - \Delta_\alpha(\omega)]^{-1}$. The multi-orbital dynamical bath function $\Delta_\alpha(\omega)$ is determined using the DMFT self-consistent condition which requires the local impurity Green function to be equal to the local Green function of the lattice (equation (3)). In equation (4), $A_{\alpha\gamma} = \frac{n_\alpha(1-2n_\alpha)+D_{\alpha\gamma}[n]}{n^0_\alpha(1-n^0_\alpha)}$ and $B_{\alpha\gamma} = \frac{(1-2n_\alpha)U_{\alpha\gamma}+\mu-\mu_\alpha}{U^2_{\alpha\gamma}n^0_\alpha(1-n^0_\alpha)}$. Here, n_α and n^0_α are particle numbers determined from G_α and G^0_α respectively, and $D_{\alpha\gamma}[n] = \langle n_\alpha n_\gamma\rangle$ is the two-body correlation function. Our interpolative *ansatz* for the self-energy is a natural extension of the IPT method for the one-orbital case, where the self-energy for each orbital α is chosen by fixing the parameters $A_{\alpha\gamma}$ and $B_{\alpha\gamma}$ such that strict compliance with the Friedel–Luttinger sum rule at $T = 0$ (guaranteeing correct low-energy behaviour) and with the first moments of the spectral function (guaranteeing correct high-energy behaviour) is maintained [12]. However, in contrast to the one-band case [14], the atomic limit for the multi-orbital case contains the local, inter-orbital correlation function, $D_{\alpha\gamma}[n] = \langle n_\alpha n_\gamma\rangle$ [15, 16] which is calculated using $\langle n_\alpha n_\gamma\rangle = \langle n_\alpha\rangle\langle n_\gamma\rangle - \frac{1}{U_{\alpha\gamma}\pi}\int_{-\infty}^{+\infty} f(\omega)\,\mathrm{Im}[\Sigma_\alpha(\omega)G_\alpha(\omega)]\,\mathrm{d}\omega$ [12]. At this point we would like to add that incorporation of the inter-orbital correlation functions is an important aspect towards novel interpolative schemes which allows one to treat the multi-orbital Anderson impurity problem in the whole range of parameters [17]. Indeed, it was already known from the seminal work of Levy Yeyati *et al* [15] that one needs to evaluate multi-orbital many-particle correlation functions to ensure a limiting form consistent with the multi-orbital atomic limit. However, apart from the implementation presented here we are aware of only one earlier work where $D_{ab}[n]$ were computed using the CPA (coherent potential approximation) [21] to obtain high-order moments.

The above *ansatz* has been successfully used to solve a host of related problems [12, 18–20], where we input the LDA DOS ($\rho^0_\alpha(\epsilon)$) into the DMFT(MO-IPT). In a multi-orbital system, DMFT leads to two effects. First, the LDA parameters like crystal field splitting are renormalized in non-trivial ways from their bare values, and may even change sign [12]. These effects result from the multi-orbital Hartree shifts, which correspond to effects captured by LDA + U. Second, and more importantly, DMFT introduces non-trivial effects stemming from the *dynamical* nature of the strong electronic correlations. Namely, these processes lead to large transfer of spectral weight across large energy scales in response to small changes in the *bare* electronic structure, a characteristic lying at the heart of the anomalous responses of correlated systems [7].

3. Numerical results and discussions

3.1. Undoped ($3d^1$) regime

Let us now present our results. In figure 1, we show the orbitally resolved spectral functions for the d_{xy} (dotted line) and the $d_{yz,zx}$ (solid) parts for $U = 3.3$ eV, with $J_H = 1.0$ eV and $U' = 1.3$ eV. Notice that rotational invariance fixes $U' = U - 2J_H$ [22]. As discussed above, DMFT results in non-trivial renormalization of the LDA crystal field splitting, $\Delta_{t_{2g}} = \epsilon_{xy} - \epsilon_\alpha$ ($\alpha \equiv yz, zx$), from -0.45 to 0.12 eV in LDA + DMFT. The occupations of the respective t_{2g} orbitals obtained from the converged solution of the dynamical mean-field equations for $U = 3.3$ eV do not differ very much from those obtained within the LDA. However, a clear charge gap showing the Mott–Hubbard character of the insulator is self-consistently generated (the very small finite DOS at $\omega = 0$ is a result of finite $T \approx 100$ K effects). The drastic change in the lineshape attests to the explicit consideration of dynamical multi-orbital correlations. Later, we will make a detailed comparison of our results with very recent photoemission spectroscopy measurements [23], showing how good qualitative agreement is obtained with reasonable parameter values. From our result, we also predict that XAS will show a shoulder feature at low-energies *above* the Mott gap, and the XAS weight will be much higher than in PES.

An important result directly gleaned from figure 1 is that $n_{d_{xy}}$:n_{d_α} = 7:3, clearly showing that the d_{xy} orbital is dominantly populated in the ground state (however, with non-negligible inter-orbital fluctuations). This is basically the condition needed to generate one-dimensional spin chains along b, as observed, and is consistent with the LDA + U [8] and (downfolded) LDA + DMFT (QMC) [11] results. Using the renormalized value of $\Delta_{t_{2g}} = 0.12$ eV along with the hopping matrix elements $t_{\alpha\beta}$ [9] and U, U', J_H as given above, the effective superexchange constant between nearest-neighbour ($S = 1/2$) spins on Ti^{4+} ions along b can be estimated. Following [24], we get $J \simeq 0.06$ meV $\widetilde{=}$ 720 K, in nice agreement with the dc susceptibility data. This is the dominant contribution to the superexchange, and we found that further-neighbour couplings are negligible on the scale of J. Given this observation, the spin–Peierls instability observed at $T_{SP} = 66$ K is almost certainly caused by coupling to lattice degrees of freedom, and *not* by competing, appreciable next-nearest-neighbour interactions [9]. The derivation of this instability is likely to involve low-dimensional effects close to and above T_{SP} and is out of the scope of *any* mean-field theory. However, we stress that the spin–Peierls transition arises as a (lattice coupling induced spontaneous breaking of translational symmetry along b) instability of the (high-T) Mott insulator derived above. This can be verified, for example, by studying the evolution of the dc spin susceptibility upon adding a small number of non-magnetic impurities at Ti sites: in analogy to $V_{1-x}Cr_xO_2$ [7], we predict a Curie component growing with the impurity concentration, which should not be observed if the I-phase is a band-Peierls insulator.

3.2. Effects of doping

We now consider the effect of carrier doping: at the outset, we clarify that attempts to dope TiOCl have not succeeded to date. On the other hand, the fact that related systems like Li_xZrNCl and M_xHfNCl (M = Li, Na) [2, 25] have been shown to become metallic and superconducting upon *electron* doping suggests that attempts to use similar strategies in TiOCl may work[4]. With this caveat, we have studied the issue of carrier density driven I–M (Mott) transition(s) in our LDA + DMFT study.

[4] Also interesting is Li_xTiNCl, which has been obtained by electrochemical Li intercalation. See [26].

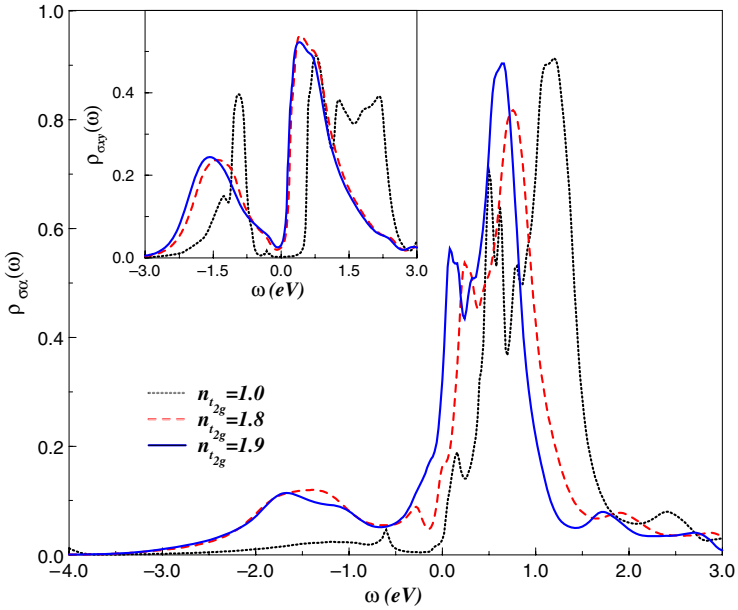

Figure 2. t_{2g} partial DOS for the $3d_{xz;yz}$ and $3d_{xy}$ (inset) orbital for different values of the total electron number.

We have repeated the LDA + DMFT calculation for electron doping (x), corresponding to band filling $n_{t_{2g}} = 1 + x$. Upon electron doping, a continuous Mott transition to a bad-metallic state is immediately observed. Further, a nearly first-order I–M transition with rapid change in the carrier density around $n_{t_{2g}} = 1.9$ is clearly seen in the LDA + DMFT results. Indeed, in TiOCl, e^--doping necessarily involves doping the d_α bands. This finding has a natural interpretation in a multi-orbital Mott–Hubbard picture. Upon addition of *electrons* to the Mott insulator (in our calculation, we change the electron number to $n_{t_{2g}} = 1 + x$ and search for the I–M instability starting from the Mott insulator found above), these prefer to occupy the higher (d_α) orbitals to escape the large (U) cost for doubly occupied d_{xy} orbitals ($U' < U$). In this situation, the renormalized $\Delta_{t_{2g}} = 0.12$ Mott insulator (MI) changes upon doping by an amount related to U' and to the self-consistently calculated average occupations $n_{xy,\alpha}$ of each t_{2g} orbital. This in turn changes $\Delta_{t_{2g}}$. More importantly, the *dynamical* multi-orbital correlations (U, U', J_H) react drastically to this small change in $\Delta_{t_{2g}}$, transferring spectral weight over large energy scales from high to low energies, and driving a Mott I–M transition at a critical x, as shown in figure 2. We clearly observe that *only* the d_α bands show metallic behaviour; the d_{xy} DOS still represents almost insulating behaviour. This is a direct consequence of the fact that it is the d_{xy} orbital which is predominantly occupied in the MI. In this limit, the multi-orbital Hartree shift for the d_α orbitals pulls the d_α states lower, populating them more (given the constraint), driving more spectral weight transfer from high to low energy (MO-DMFT), self-consistently generating a metallic state. The renormalized value of $\Delta^{M}_{t_{2g}} = -0.011$ in the metallic ($n_{t_{2g}} = 1.9$) state should imply a 'melting' of the spin dimerization observed in the I phase. More importantly, it also implies a drastic change in occupation of the various t_{2g} orbitals, corresponding to the sign change in $\Delta_{t_{2g}}$. The situation seems to be similar to the one encountered in VO_2 [27]. In the Ginsburg–Landau picture of the MIT, $\Delta_{t_{2g}}$ plays the role of an external field in the orbital sector, which drives changes in orbital occupations, leading to the

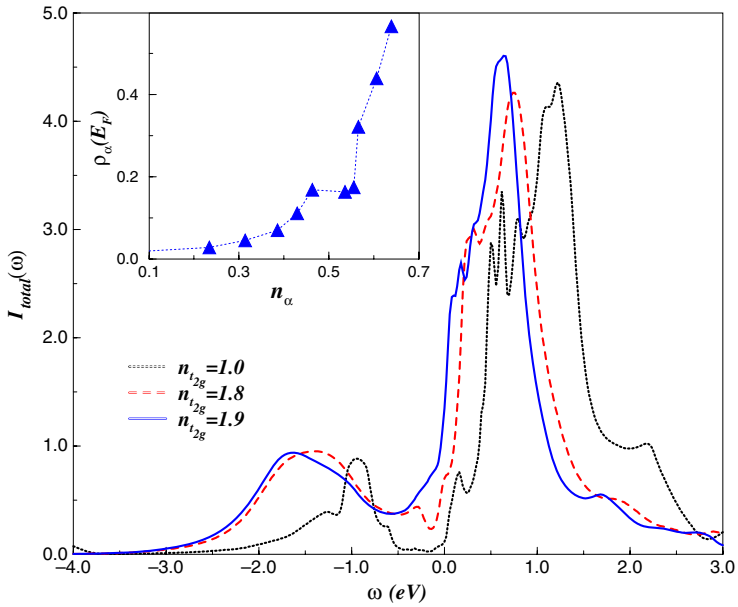

Figure 3. Total one-electron spectra for different values of the total electron number. The inset shows the $3d_{xz:yz}$ DOS at E_F as a function of the corresponding orbital occupation.

MIT via spectral weight transfer (corresponding to the second solution of the DMFT equations) beyond a critical x-dependent value.

The case of hole doping is very different: holes will predominantly occupy the lowest d_{xy} orbitals. The multi-orbital Hartree shift is now ineffective. Given the quasi-1D character of the hopping involving d_{xy} orbitals in pure TiOCl, the doped holes would be immediately localized by disorder: this is an effect which will operate at least above a certain temperature scale where the system would behave quasi-one-dimensionally [23].

In figure 3, we show the total spectra in the insulating and metallic phases. We clearly see the low-energy pseudogap in the DOS for the bad-metallic case ($n_{t_{2g}} < n_{cr} = 1.8$) and an abrupt change to a much more itinerant (large DOS at low energy) metal for $n_{t_{2g}} > n_{cr}$. Large spectral weight transfer from high energies to the Fermi level as a function of electron doping is also clearly visible. As remarked earlier, such a dynamical spectral weight driven I–M transition is out of the scope of the LDA or LDA + U methods, and can only be reliably studied within LDA + DMFT. To further explore the non-rigid-band scenario across the insulator–metal transition, we show the change in $\rho_\alpha(E_F)$ as a function of n_α (inset of figure 3) for our chosen parameter set. Clearly, $\rho_\alpha(E_F)$ jumps sharply from 0.17 to 0.31 around $n_\alpha = 0.56$, indicating an unconventional electron-doped first-order transition. Our results imply that the metallic state of TiOCl is accompanied by a jump in the itinerant carrier density at a critical value of the n_α orbital occupation close to the I–M transition. Based on our calculation, we tentatively suggest that suitably intercalated (electron-doped) TiOCl may also exhibit unconventional superconductivity upon metallization. Further, given the multi-band character of the metallic state found above, multi-band spin triplet ($J_H > \Delta_{t_{2g}}$) superconductivity may be realized in such systems. This issue is out of the scope of this paper, however, and is currently under investigation.

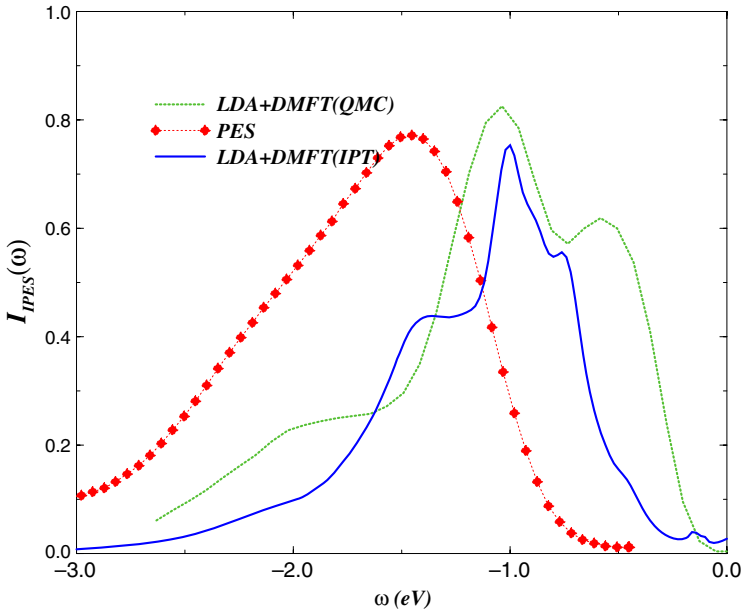

Figure 4. Comparison of two different LDA + DMFT results for the total one-electron spectral function in the insulating phase of TiOCl. The experimental result of PES taken from [23] is also shown. The LDA + DMFT (QMC) result is taken from [11]. All figures have been normalized to the same integrated area below the Fermi level[5].

3.3. Comparison between theory and experiment

To compare theoretical (LDA + DMFT) results to published experimental data [23], we repeat our calculation for $n_{t_{2g}} = 1$ using $U = 4.0$ eV, $J_H = 0.5$ eV. Here, we shall notice that the LDA + DMFT (QMC) work by Saha-Dasgupta *et al* [11] derives the many-body density of states with $U = 4.0$ eV, $J_H = 0.5$ eV. This choice implies a larger $U' = 3.0$ eV, which in turn increases the Mott–Hubbard gap in the multi-orbital problem. In figure 4 we show our result for the one-electron spectral function along with QMC [11] and the experimental [23] results taken from published literature. As one can see, noticeable changes relative to results in figure 1 are observed. In particular, the large peak around -1.0 eV (for $U = 3.3$ eV) broadens and shifts slightly to lower binding energy for $U = 4.0$ eV. There is an appreciable modification of the lineshape, as expected. These differences are important when a comparison with experiment is attempted; this is what we turn to next.

The LDA + DMFT (QMC) result has already been compared to experiment in [23]. Looking at the identical DOS results published in [11] and used to compare with experimental ones in [23], we find that a good fit to the leading edge of the PES spectrum is only possible upon a downward shift of the QMC curve by 0.66 eV. We now compare our result for $U = 4$ eV to experiment. To begin with, we notice that the position of the Fermi level inside the Mott–Hubbard gap is arbitrary, implying that it can be fixed anywhere inside the gap. Since the position of the Fermi level in an insulator can be freely chosen *inside* the Mott gap, we shift (which is consistent with the size of the Mott–Hubbard gap) the experimental result upwards by 0.41 eV and the QMC result downwards by 0.3 eV (less than the shift employed in Hoinkis *et al*

[5] Notice that in our MO-IPT calculation appreciable (36%) spectral weight is found at energies below -3.5 eV due to strong O_{2p}–t_{2g} hybridization.

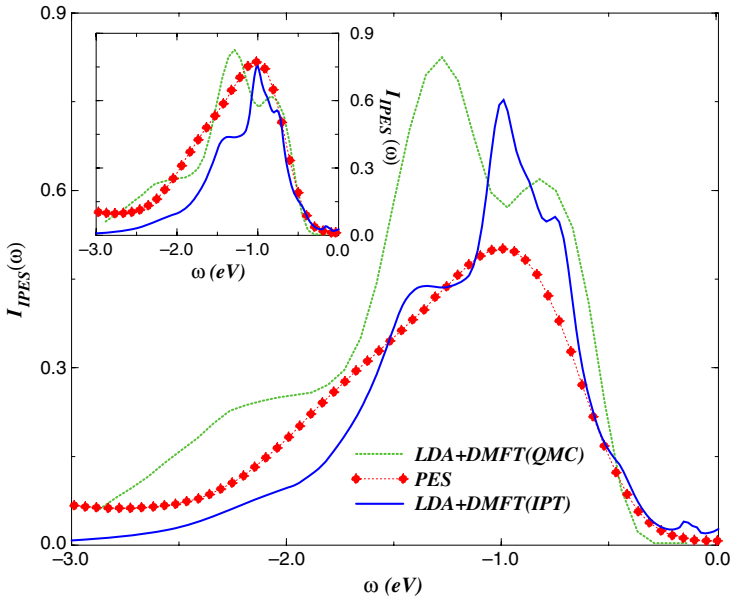

Figure 5. Comparison of two different LDA + DMFT results for the total one-electron spectral function in the insulating phase of TiOCl to the experimental results of PES taken from [23]. The LDA + DMFT (QMC) result is taken from [11]. The QMC and the experimental result have been shifted (see the text) to facilitate the comparison. Main panel: experimental data are normalized to the same integrated area as obtained within the LDA + DMFT (MO-IPT) scheme in the energy range up to −3.0 eV. Inset: all figures have been normalized to the same integrated area (see footnote 5).

work [23]). The result of following this procedure is displayed in figure 5. As one can see in the inset of this figure, where all curves have been normalized to have the same integrated weight as done in [23], good agreement with experiment over the range $-0.75 \leqslant \omega \leqslant 0$ eV is observed in both IPT and QMC solutions. Given the intrinsic uncertainty in comparing theoretical results with experimental data (because experimental data are often accompanied by some amount of surface and 'background' contributions, which is very difficult to include in the LDA + DMFT theory [20]), in the main panel of figure 5 the experimental curve is normalized such that it has the same area as the IPT one up to 3 eV binding energy. This normalization is consistent with transfer of spectral weight due to covalence effects; see figure 1. It is clear from figure 5 that within DMFT the redistribution of spectral weight due to covalence affects mainly the one-particle spectra at high energies. On the other hand, we see in figure 5 that both QMC and IPT schemes correctly account for low-energy excitations including the leading edge of the spectra. In this respect one should notice, for example, that both LDA + DMFT solutions resolve a feature at −0.76 eV (though it is much less pronounced in IPT) which has not been found experimentally. This result demonstrates the strength of QMC and IPT impurity solvers in resolving many-particle charge excitations of real multi-orbital correlated electron systems.

Notwithstanding the agreement referred to above, several comments are in order. We know that TiOCl is a spin-dimerised Mott insulator, like insulating VO_2. One would expect inter-site dynamical correlations to be non-negligible in such a situation, at least in the Mott insulating phase [28]. Generically, these correlations increase the Mott–Hubbard gap, producing significant spectral changes (in comparison with DMFT) at low energies. Clearly, such an effect cannot be treated by any single-site theory, including LDA + DMFT. In this

connection, we stress that the single-site DMFT will always yield a smaller gap compared to experiment for such a case. Finally, we shall notice that quantitative comparison with PES requires an extension of DMFT to treat the dynamical effects arising from short-ranged, intersite (dimer) correlations, and is being studied.

4. Conclusions

To conclude, we have studied the insulating state in TiOCl using the *ab initio* LDA + DMFT. In good agreement with the dc susceptibility measurement, we found that the nearest-neighbour superexchange $J \simeq 720$ K (it is 660 K in the experiment). A consistent derivation of the spin–Peierls instability from the Mott insulator requires inclusion of additional (non-local?) coupling to the lattice, and is planned for the future. In accordance with pressure studies, we found no I–M transition occurring under pressure in TiOCl. Building on this agreement with various basic observations in the I-phase of TiOCl, we suggest that electron doping the Mott insulator (this may be achievable by intercalation with suitable species) would drive a first-order Mott–Hubbard transition to a correlated metallic state. Our results show that if this transition be first order, it will be accompanied by discontinuous changes in orbital occupations, a feature which is also seen in an increasing variety of correlated, multi-orbital systems undergoing Mott transitions. Our work calls for studies on suitably intercalated TiOCl to look for possible routes to metallization and unconventional superconductivity.

Acknowledgments

We thank T Saha-Dasgupta and R Valenti for providing the LDA DOS and M Grüninger for useful discussions in the early stages of this work. The work of LC was carried out under the auspices of the Sonderforschungsbereich 608 of the Deutsche Forschungsgemeinschaft. MSL acknowledges financial support from the EPSRC (UK).

References

[1] Beynon R J and Wilson J A 1993 *J. Phys.: Condens. Matter* **5** 1983
[2] Weht R, Filippetti A and Pickett W E 1999 *Europhys. Lett.* **48** 320
[3] Rückam R, Baier J, Kriener M, Haverkort M W, Lorenz T, Uhrig G S, Jongen J, Möller A, Meyer G and Grüninger M 2005 *Phys. Rev. Lett.* **95** 097203
[4] Shaz M, van Smaalen S, Palatinus L, Hoinkis M, Klemm M, Horn S and Claessen R 2005 *Phys. Rev.* B **71** 100405(R)
[5] Caimi G, Degiorgi L, Kovaleva N N, Lemmens P and Chou F C 2004 *Phys. Rev.* B **69** 125108
Lemmens P, Choi K Y, Caimi G, Degiorgi L, Kovaleva N N, Seidel A and Chou F C 2004 *Phys. Rev.* B **70** 134429
[6] Kataev V, Baier J, Moeller A, Jongen L, Meyer G and Freimuth A 2003 *Phys. Rev.* B **68** 140405
[7] Imada M, Fujimori A and Tokura Y 1998 *Rev. Mod. Phys.* **70** 1039
[8] Seidel A, Marianetti C A, Chou F C, Ceder G and Lee P A 2003 *Phys. Rev.* B **67** 020405
[9] Saha-Dasgupta T, Valenti R, Rosner H and Gros C 2004 *Europhys. Lett.* **67** 63
[10] Pisani L and Valenti R 2005 *Phys. Rev.* B **71** 180409(R)
[11] Saha-Dasgupta T, Lichtenstein A and Valenti R 2005 *Phys. Rev.* B **71** 153108
[12] Craco L, Laad M S and Müller-Hartmann E 2003 *Phys. Rev. Lett.* **90** 237203
Laad M S, Craco L and Müller-Hartmann E 2003 *Phys. Rev. Lett.* **91** 156402
[13] Koepernik K and Eschrig H 1999 *Phys. Rev.* B **59** 1743
[14] Potthoff M, Wegner T and Nolting W 1997 *Phys. Rev.* B **55** 16132
[15] Levy Yeyati A, Flores F and Martín-Rodero A 1999 *Phys. Rev. Lett.* **83** 600
[16] Pou P, Pérez R, Flores F, Levy Yeyati A, Martin-Rodero A, Blanco J M, García-Vidal F J and Ortega L 2000 *Phys. Rev.* B **62** 4309
[17] Kotliar G, Savrasov S Y, Haule K, Oudovenko V S, Parcollet O and Marianetti C A 2006 *Rev. Mod. Phys.* **78** 865

[18] Craco L, Laad M S, Leoni S and Müller-Hartmann E 2004 *Phys. Rev.* B **70** 195116
[19] See, for example, Laad M S, Craco L and Müller-Hartmann M 2004 *New J. Phys.* **6** 157
Laad M S, Craco L and Müller-Hartmann M 2006 *Phys. Rev.* B **73** 045109
[20] Laad M S, Craco L and Müller-Hartmann M 2005 *Europhys. Lett.* **69** 984
[21] Anisimov V I, Poteryaev A I, Korotin M A, Anokhin A O and Kotliar G 1997 *J. Phys.: Condens. Matter* **9** 7359
[22] Held K and Vollhardt D 1998 *Eur. Phys. J.* B **5** 473
Pchelkina Z V, Nekrasov I A, Pruschke Th, Sekiyama A, Suga S, Anisimov Vi and Vollhardt D 2006 *Preprint* cond-mat/0601507
See also de' Medici L, Georges A and Biermann S 2005 *Preprint* cond-mat/0503764 and the references therein
[23] Hoinkis M, Sing M, Schaefer J, Klemm M, Horn S, Benthien H, Jeckelmann E, Saha-Dasgupta T, Pisani L, Valenti R and Claessen R 2005 *Phys. Rev.* B **72** 125127
[24] Mochizuki M and Imada M 2003 *Phys. Rev. Lett.* **91** 167203
[25] Yokoya T, Ishiwata Y, Shin S, Shamoto S, Iizawa K, Kajitani T, Hase I and Takahashi T 2001 *Phys. Rev.* B **64** 153107
[26] Kuhn A, Hoppe H, Strahle S and Garcia-Alvarado F 2004 *J. Electrochem. Soc.* **151** A843
[27] Laad M S, Craco L and Müller-Hartmann E 2005 *Europhys. Lett.* **69** 984
[28] Biermann S, Poteryaev A, Lichtenstein A I and Georges A 2005 *Phys. Rev. Lett.* **94** 026404